Microporous and Mesoporous Materials 125 (2009) 97–100

Contents lists available at ScienceDirect

Microporous and Mesoporous Materials

journal homepage: www.elsevier.com/locate/micromeso

A Molecular Dynamics investigation of the influence of framework flexibility on self-diffusivity of ethane in Zn(tbip) frameworks

K. Seehamart [a], T. Nanok [a], R. Krishna [b], J.M. van Baten [b], T. Remsungnen [c], S. Fritzsche [a,*]

[a] Department of Molecular Dynamics/Computer Simulation, Faculty of Physics and Geosciences, Institute for Theoretical Physics (ITP), University of Leipzig, Postfach 100920, 04009 Leipzig, Germany
[b] Van't Hoff Institute for Molecular Sciences, University of Amsterdam, Nieuwe Achtergracht 166, 1018 WV Amsterdam, The Netherlands
[c] Department of Mathematics, Faculty of Science, Khon Kaen University, Khon Kaen 40002, Thailand

ARTICLE INFO

Article history:
Received 17 November 2008
Received in revised form 29 December 2008
Accepted 15 January 2009
Available online 27 January 2009

Keywords:
Self-diffusivity
Adsorption
Molecular Dynamics
Configurational-Bias Monte Carlo
Thermodynamic factor
Framework flexibility
Isotherm inflection
Ethane
Metal-organic frameworks

ABSTRACT

Configurational-Bias Monte Carlo simulations of the adsorption isotherm of ethane in Zn(tbip) (H_2tbip = 5-tert-butyl isophthalic acid), a representative of metal-organic frameworks, show an inflection at a loading, $q_i = 6$ molecules per unit cell. This inflection causes the inverse thermodynamic factor, $1/\Gamma_i$, to display a minimum at $q_i = 6$, along with a maximum at $q_i \approx 10$. Molecular Dynamics (MD) simulations of the self-diffusivity $D_{i,self}$, taking account of the framework flexibility of Zn(tbip) show that the $D_{i,self} - q_i$ dependence follows that of $1/\Gamma_i - q_i$, with a minimum at $q_i = 6$. Remarkably, MD simulations assuming a rigid framework yield significantly lower values of the self-diffusivities, and show a monotonic decrease of $D_{i,self}$ with q_i.

1. Introduction

Metal-organic frameworks (MOFs) are a new class of porous materials that consist of metal atoms that are connected by organic linkers. In recent years there has been a significant increase in research on MOFs in view of several potential applications in the field of storage [1–3], and also separation of a variety of mixtures [4–17]. Due to the wide variety of pore sizes, and pore geometries a number of interesting separation possibilities are possible with MOFs. For the development of separation technologies utilizing MOFs, it is essential to have data and insights into the adsorption and diffusion of guest molecules. Both experimental and molecular simulation studies have shown the adsorption characteristics of a variety of guest-MOF host combinations to be rather complex and often exhibiting inflection characteristics in the isotherm, caused due to the existence of different adsorption sites of significantly varying strengths [18–24]. The number of experimental studies on diffusion in MOFs is very limited, and all published work that we are aware of emanate from Kärger's group at Leipzig [24–26]. Particularly noteworthy is the recent work of Kärger and co-workers [24], who investigated diffusion of a variety of alkanes in CuBTC ($Cu_3(BTC)_2$ where BTC = benzene-1,3,5-tricarboxylate) using infrared microscopy (IRM) and showed that the dependence of the Maxwell–Stefan (M–S) diffusivity, $Đ_i$, on the loading within CuBTC, q_i, has the same characteristics as the dependence of the $1/\Gamma_i$ on q_i, where Γ_i is the thermodynamic factor defined as:

$$\Gamma_i \equiv \frac{d \ln f_i}{d \ln q_i} \tag{1}$$

The Γ_i is obtained by differentiation of the adsorption isotherm that relates the loading q_i on the gas phase fugacity f_i. In the special case of a single-site Langmuir isotherm, the thermodynamic factor is given by:

$$\Gamma_i = \frac{1}{1 - q_i/q_{i,sat}} = \frac{1}{1 - \theta_i} \tag{2}$$

where θ_i is the fractional occupancy. The inverse thermodynamic factor $1/\Gamma_i$ can be interpreted as the generalized expression for the fractional *vacancy* that is available for the molecules to hop to within the framework. A further noteworthy feature of the work of Kärger and co-workers [24] is the demonstration that the IRM experimental results could be supported, at least at a qualitative level, by a combination of molecular simulation techniques: Configu-

* Corresponding author. Tel.: +49 0341 235 2261; fax: +49 0341 235 2307.
E-mail address: siegfried.fritzsche@uni-leipzig.de (S. Fritzsche).

1387-1811/$ - see front matter © 2009 Elsevier Inc. All rights reserved.
doi:10.1016/j.micromeso.2009.01.020

Nomenclature

Notation

$Đ_i$	Maxwell–Stefan diffusivity of species *i*, $m^2\ s^{-1}$
$D_{i,self}$	self-diffusivity of species *i*, $m^2\ s^{-1}$
f_i	fugacity of species *i*, Pa
q_i	loading of species *i*, molecules per unit cell
$q_{i,sat}$	saturation loading of species *i*, molecules per unit cell

Greek letters

Γ_i	thermodynamic correction factor, dimensionless
θ_i	fractional occupancy, $\theta_i = q_i/q_{i,sat}$, dimensionless

rational-Bias Monte Carlo (CBMC) simulation of adsorption isotherms, and Molecular Dynamics (MD) simulations of diffusivities. Both CBMC and MD simulations were carried out assuming a rigid framework; this assumption is probably justified for CuBTC. The link between the dependence of $Đ_i - q_i$ and $1/\Gamma_i - q_i$ has been shown in several molecular simulation studies in zeolites [27–30], again assuming a *rigid* zeolite framework. For example, for diffusion of isobutane (iC4) in MFI zeolite, Kinetic Monte Carlo (KMC) simulations predict a sharp minimum in both the M–S diffusivity $Đ_i$, as also the self-diffusivity, $D_{i,self}$, at $q_i = 4$ molecules per unit cell, corresponding to the loading at which isotherm inflection occurs [28]. In another pioneering experimental study, Kärger and co-workers [31] have performed IRM experiments to confirm the anticipations of the KMC simulations.

In recent MD investigations of diffusion in IRMOF-1 [32,33], it has been shown that the framework flexibility has a profound influence diffusion of guest molecules in MOFs. Amirjalayer et al. [32] have found that the self-diffusivity for benzene in IRMOF-1 in the simulations with rigid lattice was larger than with a flexible lattice. This finding is surprising because a rigid lattice can be expected to restrict the motion of the guest molecule more than a flexible framework.

The major objective of the present communication is to investigate, using molecular simulation techniques, the influence of framework flexibility on the dependence of the diffusivity on the loading q_i. For illustration purposes we have chosen Zn(tbip) (H_2tbip = 5-tert-butyl isophthalic acid) as the framework structure, in view of the high thermal stability and gas separation capability [5,6]. The guest molecule is chosen to be ethane (C2) because of the inflection behaviour in the isotherm, as we shall see later. We aim to show that framework flexibility has not only a quantitative influence on the diffusivity values, but the loading dependence is also *qualitatively* affected.

The details of the CBMC and MD simulation methodologies, along with the details of the force fields used for fixed and flexible Zn(tbip) frameworks are provided in the Supplementary material accompanying this publication. The major simulation results are discussed below.

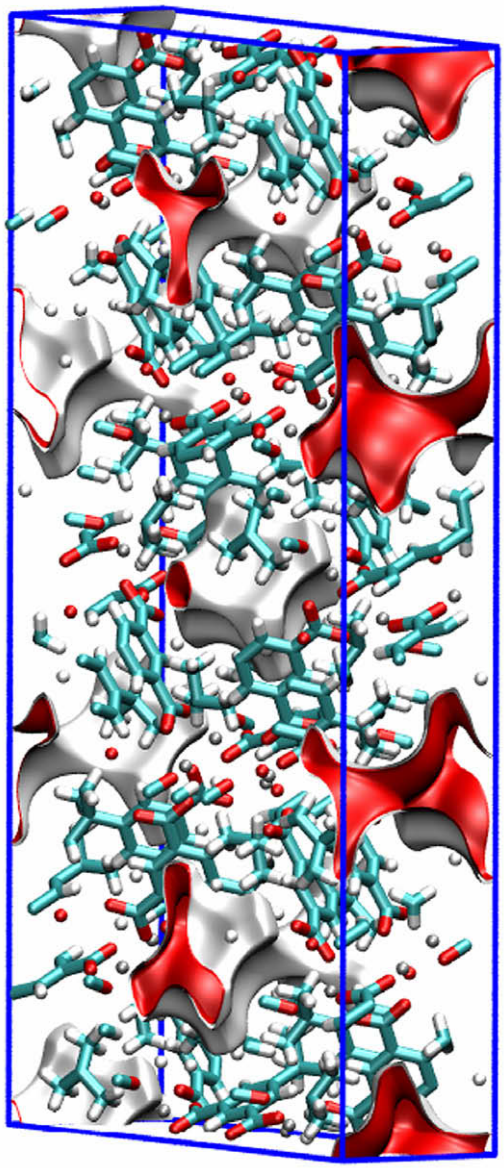

Fig. 1. Perspective view of one unit cell of Zn(tbip), along with landscape (isopotential surfaces) of channels.

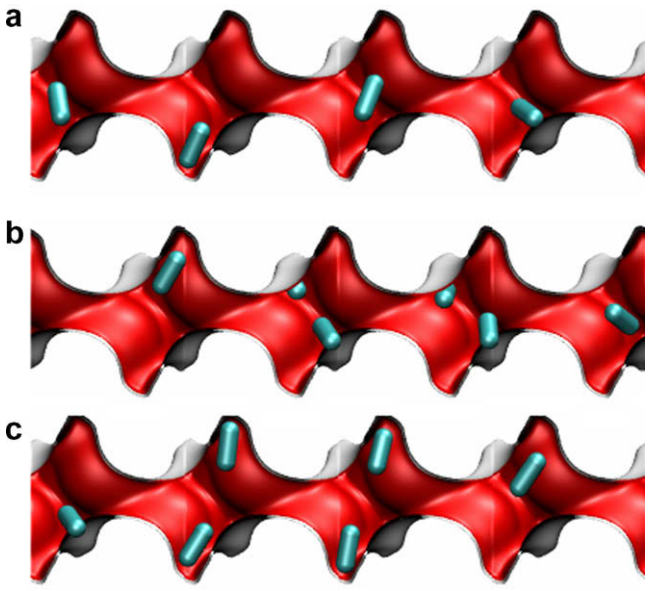

Fig. 2. Snapshots showing the location of ethane molecules within the one-dimensional channels of Zn(tbip) for loadings of (a) $q_i = 6$, (b) $q_i = 8$, and (c) $q_i = 12$ molecules per unit cell. The view shows four unit cells in the *z*-direction.

2. Simulation results, discussions, and conclusions

Fig. 1 gives a perspective view of one unit cell of Zn(tbip). Each unit cell consist a total of six channel segments. At low pressures a maximum of one ethane molecule can occupy each channel segment; only at higher pressures is it possible to locate more than one molecule per channel segment. This is evidenced by the snapshots in Fig. 2a–c showing the location of ethane molecules within the one-dimensional channels of Zn(tbip) for loadings of $q_i = 6$, 8, and 12 molecules per unit cell, respectively. CBMC simulations of the adsorption isotherms for C2 in Zn(tbip) at 300 K are shown in Fig. 3a. The adsorption isotherm shows an inflection at a loading of six molecules per unit cell, i.e., corresponding to a loading of one molecule per channel segment. This implies that an extra "push", i.e., additional pressure, is required to locate more than one molecule per segment. This extra push is the root cause of the inflection in the isotherm. For a good description of the complete isotherm, a dual-site Langmuir fit is required; this fit is shown by the continuous solid line in Fig. 3a. The inverse thermodynamic factor $1/\Gamma_i$, obtained by analytic differentiation of the dual-site Langmuir fit is shown in Fig. 3b. The minimum of $1/\Gamma_i - q_i$ curve at $q_i = 6$ is noteworthy, as also the near-flat maximum at $q_i \approx 10$. In the range $0 < q_i < 6$, $1/\Gamma_i$ decreases nearly linearly with q_i signifying the fact that the vacancy decreases almost linearly with loading. For $6 < q_i < 10$, $1/\Gamma_i$ increases with q_i because additional sites within the channel segments are created to accommodate more than one molecule per segment, i.e., the available sites increase within this loading range.

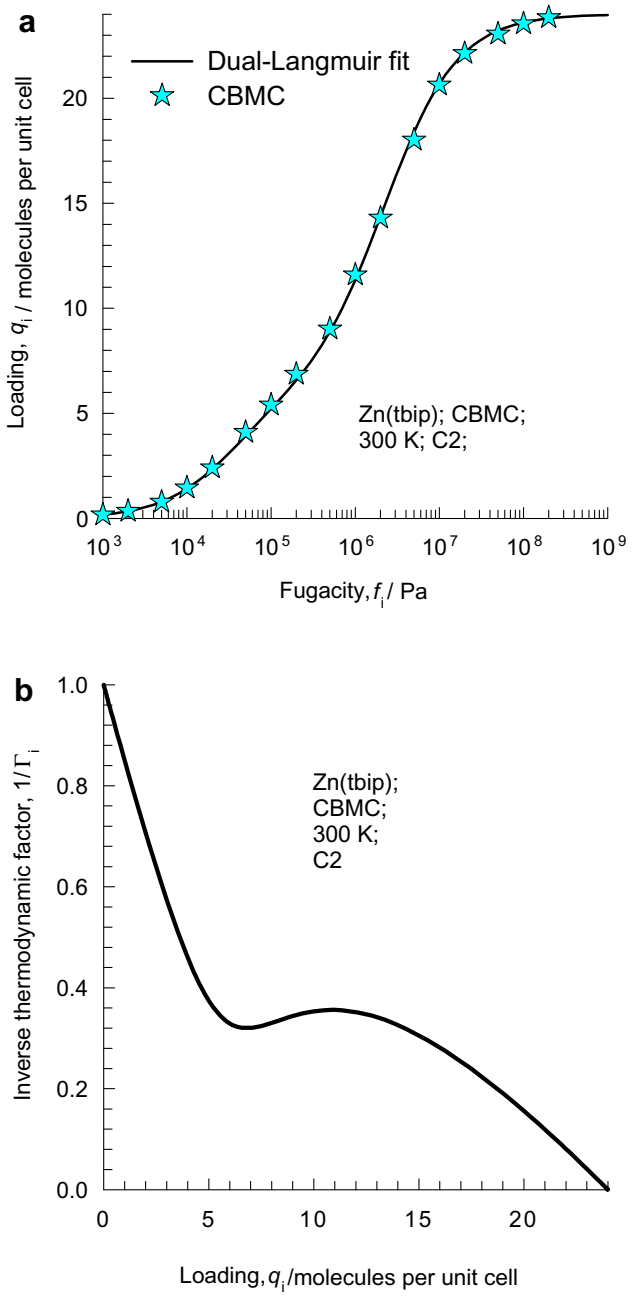

Fig. 3. (a) CBMC simulations of the adsorption isotherm for C2 in Zn(tbip) at 300 K. The continuous solid line is the dual-site Langmuir fit of the isotherm (fit parameters are given in the Supplementary material) and (b) the inverse thermodynamic factor $1/\Gamma_i$ obtained by differentiation of the dual-site Langmuir fit at 300 K.

Diffusion in Zn(tbip) is essentially *z*-dimensional and the reported diffusivities are along this direction. Fig. 4 shows the MD simulations for the self-diffusivity $D_{i,self}$ as a function of the loading, q_i. In the loading range $0 < q_i < 6$, both fixed and flexible framework results yields a near-linear decline in the diffusivity with loading; this is because the vacancy decreases linearly with loading in this range. The results assuming a rigid framework yield significantly lower values of $D_{i,self}$ than the corresponding results with a flexible framework; the differences between the two sets of values is about a factor 10 at high q_i. There are *qualitative* differences between the two sets of results for $q_i < 6$. The fixed framework results show a monotonic decrease of $D_{i,self}$ with q_i. The flexible framework results appear to follow the trend shown by the $1/\Gamma_i - q_i$ curve with a sharp minimum at a loading of six corresponding to the isotherm inflection point; for loadings in excess of six molecules per unit cell, the $D_{i,self}$ increases with q_i, reaching a maximum at a loading of approximately nine molecules per unit cell, in qualitative agreement with the dependence of $1/\Gamma_i$. The increase in the diffusivity for $6 < q_i < 9$ is because additional adsorption sites are created within each channel segment and the diffusivity increase is because there are more vacant sites for the molecules to hop to. Apparently, the accommodation of greater than one molecule per channel segment is easier with a flexible framework, than in a fixed framework.

Our work underlines the need for taking the flexibility of the framework into consideration in diffusion simulations, but the precise reason for the qualitative differences in the diffusion

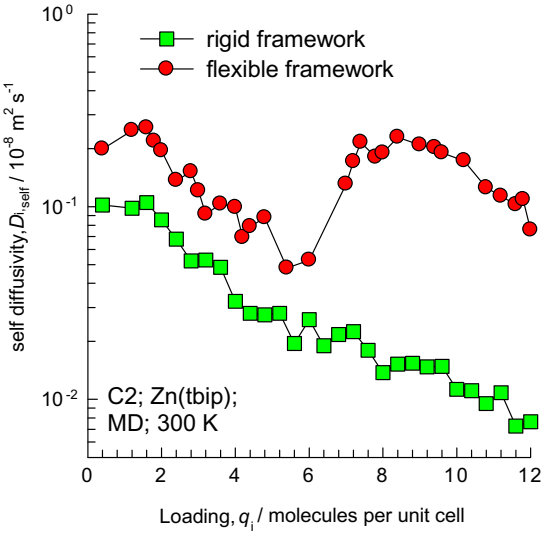

Fig. 4. The self-diffusion coefficients of ethane as a function of loading, for both flexible and rigid frameworks.

characteristics with fixed and flexible frameworks needs further investigation.

Acknowledgements

S. Fritzsche gratefully acknowledges financial support from the DFG, SPP 1362. T. Nanok thanks the DFG SPP 1155 for a postdoc position. K. Seehamart thanks the Rajamangala University of Technology Isan (RMUTI) for a PhD Grant. T. Remsungnen thanks the DFG (Project FR1486/1-4) for financial support. We thank the computer center of the university Leipzig (particularly Mr. Rost who supported us) and the center for information services and high performance computing (ZIH) of Dresden University of Technology for computer facilities and CPU time. R. Krishna acknowledges the DFG for the award of a Mercator Professorship.

Appendix A. Supplementary data

Supplementary data associated with this article can be found, in the online version, at doi:10.1016/j.micromeso.2009.01.020.

References

[1] U. Mueller, M. Schubert, F. Teich, H. Puetter, K. Schierle-Arndt, J. Pastre, J. Mater. Chem. 16 (2006) 626.
[2] O.M. Yaghi, Nature Mater. 6 (2007) 92.
[3] R.Q. Snurr, J.T. Hupp, S.T. Nguyen, A.I.Ch.E.J. 50 (2004) 1090.
[4] L. Bastin, P.S. Bárcia, E.J. Hurtado, J.A.C. Silva, A.E. Rodrigues, B. Chen, J. Phys. Chem. C 112 (2008) 1575.
[5] L. Pan, D.H. Olson, L.R. Ciemnolonski, R. Heddy, J. Li, Angew. Chem. Int. Ed. 45 (2006) 616.
[6] L. Pan, B. Parker, X. Huang, D.H. Olson, J.Y. Lee, J. Li, J. Am. Chem. Soc. 128 (2006) 4180.
[7] P.S. Bárcia, F. Zapata, J.A.C. Silva, A.E. Rodrigues, B. Chen, J. Phys. Chem. B 111 (2008) 6101.
[8] B. Chen, C. Liang, J. Yang, D.S. Contreras, Y.L. Clancy, E.B. Lobkovsky, O.M. Yaghi, S. Dai, Angew. Chem. Int. Ed. 45 (2006) 1590.
[9] D.N. Dybtsev, H. Chun, S.H. Yoon, D. Kim, K. Kim, J. Am. Chem. Soc. 126 (2004) 32.
[10] V. Finsy, H. Verelst, L. Alaerts, D. De Vos, P.A. Jacobs, G.V. Baron, J.F.M. Denayer, J. Am. Chem. Soc. 130 (2008) 7110.
[11] L. Alaerts, C.E.A. Kirschhock, M. Maes, M. van der Veen, V. Finsy, A. Depla, J.A. Martens, G.V. Baron, P.A. Jacobs, J.F.M. Denayer, D. De Vos, Angew. Chem. Int. Ed. 46 (2007) 4293.
[12] Q.M. Wang, D. Shen, M. Bülow, M.L. Lau, S. Deng, F.R. Fitch, N.O. Lemcoff, J. Semanscin, Micropor. Mesopor. Mater. 55 (2002) 217.
[13] L. Zhang, Q. Wang, T. Wu, Y.C. Liu, Chem. Eur. J. 13 (2007) 6387.
[14] S. Wang, Q. Yang, C. Zhong, Sep. Purif. Technol. 60 (2008) 30.
[15] Q. Yang, C. Xue, C. Zhong, J.F. Chen, A.I.Ch.E.J. 53 (2007) 2832.
[16] Q. Yang, C. Zhong, J. Phys. Chem. B 110 (2006) 17776.
[17] D. Dubbeldam, C.J. Galvin, K.S. Walton, D.E. Ellis, R.Q. Snurr, J. Am. Chem. Soc. 130 (2008) 10884.
[18] A. Kondo, H. Noguchi, L. Carlucci, D.M. Proserpio, G. Ciani, H. Kajiro, T. Ohba, H. Kanoh, K. Kaneko, J. Am. Chem. Soc. 129 (2007) 12362.
[19] D. Dubbeldam, H. Frost, K.S. Walton, R.Q. Snurr, Fluid Phase Equilibr. 261 (2007) 152.
[20] V. Krungleviciute, K. Lask, L. Heroux, A.D. Migone, J.Y. Lee, J. Li, A.I. Skoulidas, Langmuir 23 (2007) 3106.
[21] V. Krungleviciute, K. Lask, A.D. Migone, J.Y. Lee, J. Li, A.I.Ch.E.J. 54 (2008) 918.
[22] A. Vishnyakov, P.I. Ravikovitch, A.V. Neimark, M. Bülow, Q.M. Wang, Nano Lett. 3 (2003) 713.
[23] K.S. Walton, A.R. Millward, D. Dubbeldam, H. Frost, J.J. Low, O.M. Yaghi, R.Q. Snurr, J. Am. Chem. Soc. 130 (2008) 406.
[24] C. Chmelik, J. Kärger, M. Wiebcke, J. Caro, J.M. van Baten, R. Krishna, Micropor. Mesopor. Mater. 117 (2009) 22.
[25] F. Stallmach, S. Gröger, V. Künzel, J. Kärger, O.M. Yaghi, M. Hesse, U. Müller, Angew. Chem. Int. Ed. 45 (2006) 2123.
[26] P. Kortunov, L. Heinke, M. Arnold, Y. Nedellec, D.J. Jones, J. Caro, J. Kärger, J. Am. Chem. Soc. 129 (2007) 8041.
[27] R. Krishna, J.M. van Baten, Micropor. Mesopor. Mater. 109 (2008) 91.
[28] R. Krishna, D. Paschek, Chem. Eng. J. 85 (2002) 7.
[29] R. Krishna, J.M. van Baten, Chem. Phys. Lett. 420 (2006) 545.
[30] H. Jobic, C. Laloué, C. Laroche, J.M. van Baten, R. Krishna, J. Phys. Chem. B 110 (2006) 2195.
[31] C. Chmelik, L. Heinke, J. Kärger, D.B. Shah, W. Schmidt, J.M. van Baten, R. Krishna, Chem. Phys. Lett. 459 (2008) 141.
[32] S. Amirjalayer, M. Tafipolsky, R. Schmid, Angew. Chem. Int. Ed. 46 (2007) 463.
[33] J.A. Greathouse, M.D. Allendorf, J. Phys. Chem. C 112 (2008) 5795.

Supplementary material to accompany

A Molecular Dynamics investigation of the influence of framework flexibility on self-diffusivity of ethane in Zn(tbip) frameworks

K. Seehamart[1], T. Nanok[1], R. Krishna[2], J. M. van Baten[2], T. Remsungnen[3] and S. Fritzsche[1*]

[1]Department of Molecular Dynamics/Computer Simulation, Faculty of Physics and Geosciences, Institute for Theoretical Physics (ITP), University of Leipzig, Postfach 100920, 04009 Leipzig, Germany

[2]Van't Hoff Institute for Molecular Sciences, University of Amsterdam, Nieuwe Achtergracht 166, 1018 WV Amsterdam, The Netherlands

[3]Department of Mathematics, Faculty of Science, Khon Kaen University, Khon Kaen 40002, Thailand.

*CORRESPONDING AUTHOR: Tel 0341 235 2261; Fax: 0341 235 2307; email: siegfried.fritzsche@uni-leipzig.de

Monte Carlo simulation methodology

The structural information for Zn(tbip) simulations have been taken from Pan et al.[1]. The structure data file we used is available on our website [2]. The framework structure, along with the pore (energy) landscapes are presented in Figures 1, 2, 3, and 4. One unit cell of Zn(tbip) contains a total of six channel segments.

The adsorption isotherms were computed using Monte Carlo (MC) simulations in the grand canonical (GC) ensemble. The Configurational-Bias Monte Carlo (CBMC) simulation technique, which has been given in details elsewhere [3-6], was employed. All CBMC simulations were performed using the BIGMAC code developed by T.J.H. Vlugt[7] as basis.

The Zn(tbip) framework was considered to be rigid in the simulations. The interactions between the Zn(tbip) framework and ethane molecules were described by the 12-6 Lennard-Jones (LJ) potentials. The LJ parameters for the Zn(tbip) framework atoms were mostly taken from the work of Dubbeldam et al. [8] and partly adopted from the second generation force field of Kollman et al [9].The ethane molecule was modeled as two united atoms with a fix bond length of 1.53 Å and the LJ parameters were taken from the transferable potentials for phase equilibria (TraPPE) model [10]. The Lorentz-Berthelot mixing rules were applied for calculating σ and ε for guest-host interactions. The Lennard-Jones potentials are shifted and cut at 12 Å.

Typical snapshots showing the location of ethane molecules along the length of the channels is shown in Figures 5, 6 and 7 for loadings of 6, 8, and 12 molecules per unit cell respectively.

The CBMC simulations of the isotherm for C2 in Zn(tbip) was fitted with the dual-site Langmuir isotherm

$$q_i = q_{i,A} + q_{i,B} = \frac{q_{i,sat,A} b_{i,A} f_i}{1 + b_{i,A} f_i} + \frac{q_{i,sat,B} b_{i,B} f_i}{1 + b_{i,B} f_i} \tag{1}$$

The values of the fitted parameters are:

$$\begin{aligned} q_{i,sat,A} &= 6 \quad \text{molecules per unit cell} \\ q_{i,sat,B} &= 18 \quad \text{molecules per unit cell} \\ b_{i,A} &= 2.87 \times 10^{-5} \quad \text{Pa}^{-1} \\ b_{i,B} &= 4.45 \times 10^{-7} \quad \text{Pa}^{-1} \end{aligned} \tag{2}$$

The inverse thermodynamic factor can be calculated from

$$\frac{1}{\Gamma_i} = \frac{q_{i,A}}{q_i}\left(1 - \frac{q_{i,A}}{q_{i,A,sat}}\right) + \frac{q_{i,B}}{q_i}\left(1 - \frac{q_{i,B}}{q_{i,B,sat}}\right) \tag{3}$$

Animations

For visual appreciation of the diffusion phenomena in Zn(tbip), animations were created on the basis of the MD simulations, for both fixed and flexible frameworks; these can be viewed after downloading the movies from our website [2].

Molecular Dynamics (MD) simulation methodology

The MD simulations have been carried out with the DL_POLY simulation package. The simulation box has the dimensions of 28.863 × 49.992 × 39.855 Å^3. This contains five unit cells of Zn(tbip) and comprises of 5220 framework atoms. The periodic boundary conditions have been applied to all three directions. The long-range electrostatic interactions between the Zn(tbip) framework atoms have been computed using the Ewald method and the short-range van der Waals interactions between framework atoms and between framework and ethane

molecules have been computed up to a cutoff radius of 12 Å. The equations of motion have been integrated with the time step of 1 ns. All MD runs have been performed in the canonical *(NVT)* ensemble at a temperature of 298 K using the Nosé-Hoover thermostat.

In the case of the MD simulations with rigid lattice the initial situation for each run has been relaxed by Monte Carlo simulations while in the runs with flexible lattice this relaxation has been done by an initial thermalizing part of the run of 1-2 ns before evaluations start. After that, the production runs have been conducted for 10 ns. During the production runs, the coordinates have been stored every 100 fs for further analyses.

The force field parameters used are explained and given below.

Zn(tbip)-ethane interactions

For the interactions between the Zn(tbip) framework and ethane molecules the same 12-6 Lennard-Jones (LJ) potentials are used as for the CBMC simulations. These potential parameters are described in the MC section and they are given in Table 1.

The flexible framework of Zn(tbip)

The flexible lattice of Zn(tbip) was modeled in a similar way to the fully bonded force field of Schmid et al. [11] where the metal-oxygen interactions were treated as covalent bonds. The definitions of different atoms in the Zn(tbip) framework are shown in Figure 6. The bond stretches and bond bends were described by a simple harmonic potential function while the bond torsion and improper torsion angles were expressed by the periodic cosine potential function. The force constants which reasonably well reproduced the dynamics properties of the metal organic frameworks (MOFs) in previous literature [9, 11-13] were adopted to be used in this study. The equilibrium bond distances and angles were assigned by averaging from the experimental crystal data excepting the C-H bond distances, which seem too

contacted from the normal C-H bonds, were taken from available standard optimized structures. Electrostatic and van der Waals interactions were calculated only between atoms separated by more than three bonds. All force field parameters of the Zn(tibp) flexible framework are listed in Table 1. The nomenclature for the atoms in the Zn(tbip) framework are specified in Figure 8.

$$U^{total} = U^{bonded} + U^{nonbonde}$$

$$U^{bonded} = U^{bond} + U^{bend} + U^{torsion} + U^{imp.\ torsion}$$

$$U^{nonbonded} = U^{Coul} + U^{LJ}$$

$$U^{bond} = \tfrac{1}{2} k_r (r - r_0)^2$$

$$U^{bend} = \tfrac{1}{2} k_\theta (\theta - \theta_0)^2$$

$$U^{torsion} = k_\phi [1 + \cos(m\phi - \phi_0)]$$

$$U^{imp.torsion} = k_\phi [1 + \cos(m\phi - \phi_0)]$$

$$U^{nonbonded} = c \cdot \frac{q_i q_j}{r_{ij}} + 4\varepsilon_{ij} \left[\left(\frac{\sigma_{ij}}{r_{ij}} \right)^{12} - \left(\frac{\sigma_{ij}}{r_{ij}} \right)^{6} \right]$$

Molecule trajectories during MD simulations

In order to understand the difference between the diffusion behaviour at low and high loadings of guest molecules we have marked locations of a selected diffusing molecule every 0.5 ps during a simulation period of 10 ns at loadings of 3.2 and 8.4 ethane molecule per unit cell, respectively, with flexible lattice. The results can be seen in Figure 9. The plots in the left column visualize the density distribution of sites for the lower density (3.2). The uppermost picture shows a head-on view along the channel axis and it can be seen that the particle spends most of the time in the central part of the channel. The two lower pictures within this

column show that there exist preferred regions of residence along the channel. In the right hand side of Figure 9 it can be seen that there exist no such preferred regions at higher densities.

References

[1] L. Pan, B. Parker, X. Huang, D.H. Olson, J.Y. Lee, J. Li, Zn(tbip) (H_2 tbip)=5-*tert*-Butyl Isophthalic Acid): A Highly Stable Guest-Free Microporous Metal Organic Framework with Unique Gas Separation Capability, J. Am. Chem. Soc. 128 (2006) 4180-4181.

[2] J.M. van Baten, R. Krishna, MD animations of diffusion in nanoporous materials, University of Amsterdam, Amsterdam, http://www.science.uva.nl/research/cr/animateMD/, 5 October 2008.

[3] D. Dubbeldam, S. Calero, T.J.H. Vlugt, R. Krishna, T.L.M. Maesen, B. Smit, United Atom Forcefield for Alkanes in Nanoporous Materials, J. Phys. Chem. B 108 (2004) 12301-12313.

[4] D. Frenkel, B. Smit, Understanding molecular simulations: from algorithms to applications, Academic Press, 2nd Edition, San Diego, 2002.

[5] T.J.H. Vlugt, R. Krishna, B. Smit, Molecular simulations of adsorption isotherms for linear and branched alkanes and their mixtures in silicalite, J. Phys. Chem. B 103 (1999) 1102-1118.

[6] D. Dubbeldam, S. Calero, T.J.H. Vlugt, R. Krishna, T.L.M. Maesen, E. Beerdsen, B. Smit, Force Field Parametrization through Fitting on Inflection Points in Isotherms, Phys. Rev. Lett. 93 (2004) 088302.

[7] T.J.H. Vlugt, BIGMAC, University of Amsterdam, http://molsim.chem.uva.nl/bigmac/, 1 November 2000.

[8] D. Dubbeldam, K.S.Walton, D.E. Ellis, R.Q. Snurr, Angew. Chem. Int. Ed. 46 (2007) 4496.

[9] W.D. Cornell, P. Cieplak, C.I. Bayly, I.R. Gould, K.M. Merz, Jr., D.M. Ferguson, D.C. Spellmeyer, T. Fox, J.W. Caldwell, P.A. Kollman, J. Am. Chem. Soc. 117 (1995) 5179.

[10] M.G. Martin, J.I. Siepmann, J. Phys. Chem. B 1998, **102**, 2569.

[11] M. Tafipolsky, S. Amirjalayer, R. Schmid, J. Comput. Chem. 2007, **28**, 1169.

[12] A.K. Rappé, C. J. Casewit, K.S. Colwell, W.A. Goddard III, and W.M. Skiff, J. Am. Chem. Soc. 1992, **114**, 10024.

[13] J.A. Greathouse, M.D. Allendorf, J. Phys. Chem. C 2008, **112**, 5795.

Table 1. Force field parameters for the flexible Zn(tbip) and ethane molecule used in this study. The nomenclature for the atoms in the Zn(tbip) framework are specified in Figure 8.

Bond stretch

i-j	k_r (kJ/(mol· Å^2))	r_0 (Å)	ref.
Zn-O1	1142.041	1.941	12
O1-C1	4518.800	1.261	13
C1-C2	2939.200	1.480	13
C2-C3	4016.600	1.390	13
C2-C4	4016.600	1.390	13
C4-C5	4016.600	1.390	13
C5-C6	2652.656	1.530	9
C6-C7	2594.080	1.500	9
C3-H3	3041.000	1.080	13
C4-H4	3041.000	1.080	13
C7-H7	2845.120	1.112	9

Bond Bend

i-j-k	k_θ (kJ/(mol·rad^2))	θ_0 (degree)	ref.
O1-Zn-O1	132.484	104.5	11
O1-Zn-O1	132.484	134.6	11
Zn-O1-C1	258.946	137.0	11
Zn-O1-C1	258.946	131.0	11

O1-C1-O1	1213.400	125.0	13
O1-C1-C2	456.000	118.0	13
C1-C2-C3	290.200	120.0	13
C1-C2-C4	290.200	120.0	13
C2-C3-H3	309.600	120.0	13
C2-C4-H4	309.600	120.0	13
C2-C3-C2	753.200	120.0	13
C2-C4-C5	753.200	120.0	13
C3-C2-C4	753.200	120.0	13
C4-C5-C4	753.200	120.0	13
C4-C5-C6	585.760	120.0	9
C5-C6-C7	527.184	109.5	9
C6-C7-H7	418.000	109.5	9
C7-C6-C7	334.720	109.5	9
H7-C7-H7	292.880	109.5	9

Torsion Bend

i-j-k-l	$k_{ø}$ (kj/mol)	$ø_0$ (degree)	*m*	ref.
Zn-O1-C1-O	20.9000	180.0	2	11
Zn-O1-C1-C2	20.9000	180.0	2	11
O1-Zn-O1-C2	20.9000	180.0	2	11
O1-C1-C2-C2	10.4900	180.0	2	13
C1-C2-C3-C2	12.5520	180.0	2	13
C1-C2-C4-C5	12.5520	180.0	2	13

C1-C2-C4-H4	12.5520	180.0	2	13
C2-C3-C2-C4	12.5520	180.0	2	13
C2-C4-C5-C6	12.5520	180.0	2	13
C3-C2-C4-C5	12.5520	180.0	2	13
C3-C2-C4-H4	12.5520	180.0	2	13
C4-C2-C3-H3	12.5520	180.0	2	13
C4-C5-C4-H4	12.5520	180.0	2	13
C4-C5-C6-C7	0.0000	180.0	2	9
C5-C6-C7-H7	11.7152	0.0	3	9

Improper Torsion

i-j-k-l	$k_{ø}$ (kj/mol)	$ø_0$ (degree)	*m*	ref.
O1-O1-C1-C2	41.84	180.0	2	11
C1-C2-C3-C4	41.84	180.0	2	11
C1-C2-C4-C3	41.84	180.0	2	11
C2-C3-C2-H3	1.55	180.0	2	13
C2-C4-C5-H4	1.55	180.0	2	13
C3-C2-C4-C1	41.84	180.0	2	11
C3-C2-C1-C4	41.84	180.0	2	11
C4-C2-C3-C1	41.84	180.0	2	11
C4-C2-C1-C3	41.84	180.0	2	11
C4-C5-C4-C6	41.84	180.0	2	11
C4-C5-C6-C4	41.84	180.0	2	11
C5-C4-C2-H4	1.55	180.0	2	13

Non-bonded Interactions

atom type	ε (kJ/mol)	σ (Å)	charge (a.u.)	ref.
Zn	0.0035	2.70	1.200	8
O1	0.5862	3.11	-0.600	8
C1	0.3908	3.74	0.475	8
C2	0.3979	3.47	0.125	8
C3	0.3979	3.47	-0.15	8
C4	0.3979	3.47	-0.15	8
C5	0.3979	3.47	0.000	8
C6	0.0066	3.40	0.000	9
C7	0.4569	3.40	-0.30	9
H3	0.0636	2.85	0.150	8
H4	0.0636	2.85	0.150	8
H7	0.0656	2.65	0.100	9
$CH_{3(ethane)}$	0.8141	3.75	0.000	10

Figure captions

Figures 1-4. Structure and pore landscapes (Isopotential surfaces) of Zn(tbip).

Figure 5. Snapshot of the location of ethane molecules in the Zn(tbip). The side view of Zn(tbip) is 4 unit cells long. Total loading = 6 molecules per unit cell.

Figure 6. Snapshot of the location of ethane molecules in the Zn(tbip). The side view of Zn(tbip) is 4 unit cells long. Total loading = 8 molecules per unit cell.

Figure 7. Snapshot of the location of ethane molecules in the Zn(tbip). The side view of Zn(tbip) is 4 unit cells long. Total loading = 12 molecules per unit cell.

Figure 8. Definitions of different atoms in the Zn(tbip) framework.

Figure 9.. Trajectories of one arbitrary selected ethane molecule in a one-dimensional channel of Zn(tbip) projected into *xy*, *xz*, and *yz* planes from the simulation loadings of 3.2 (left) and 8.4 (right) molecules/unit cell. Note that the coordinate is monitored every 0.5 ps during the simulation time of 10 ns and only some part of the total length in the *z* axis is shown for clarity.

Figure 1

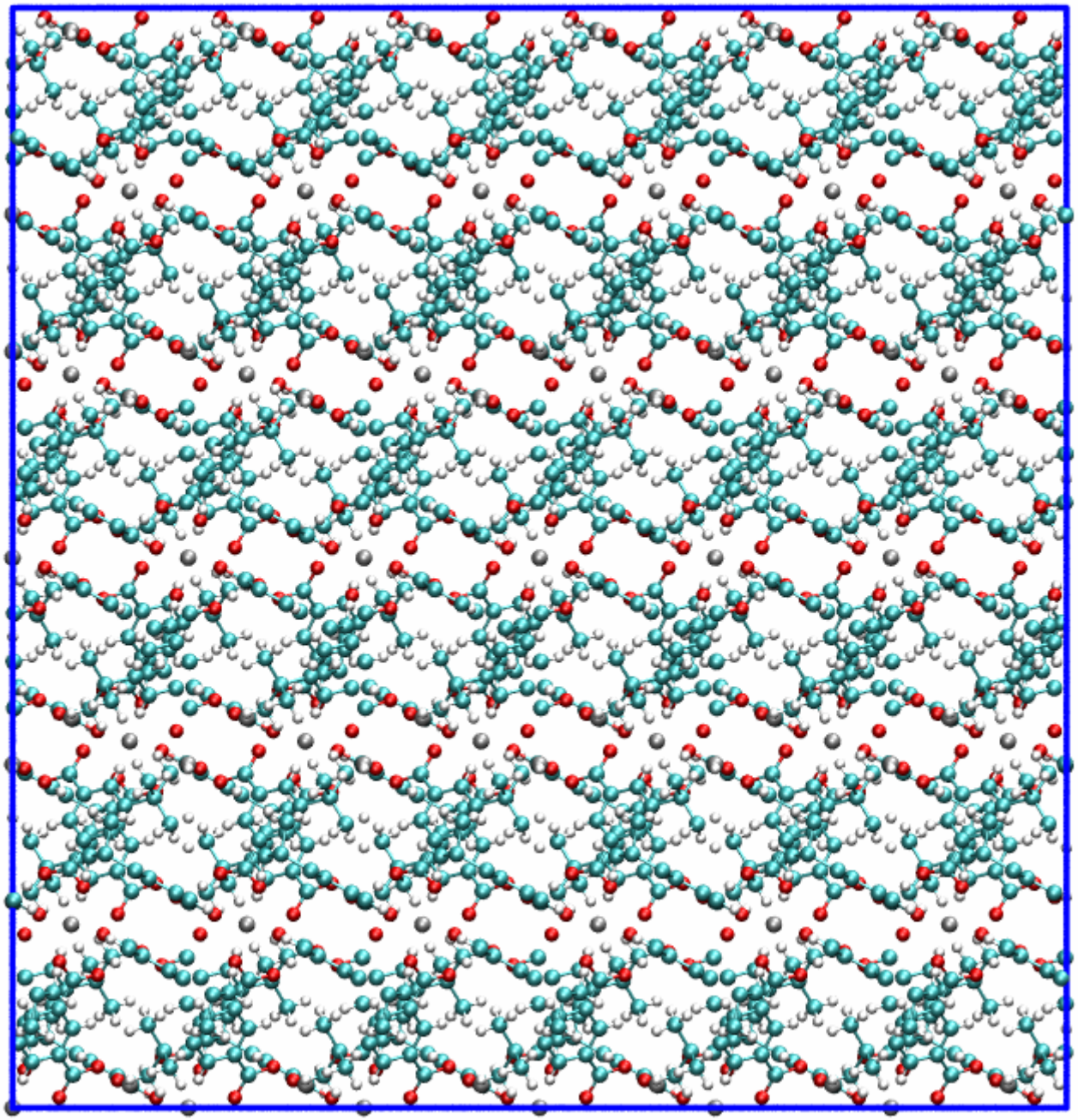

Side view of framework;
Channels from left to right

Figure 2

Head-on view of framework; Channels into the paper

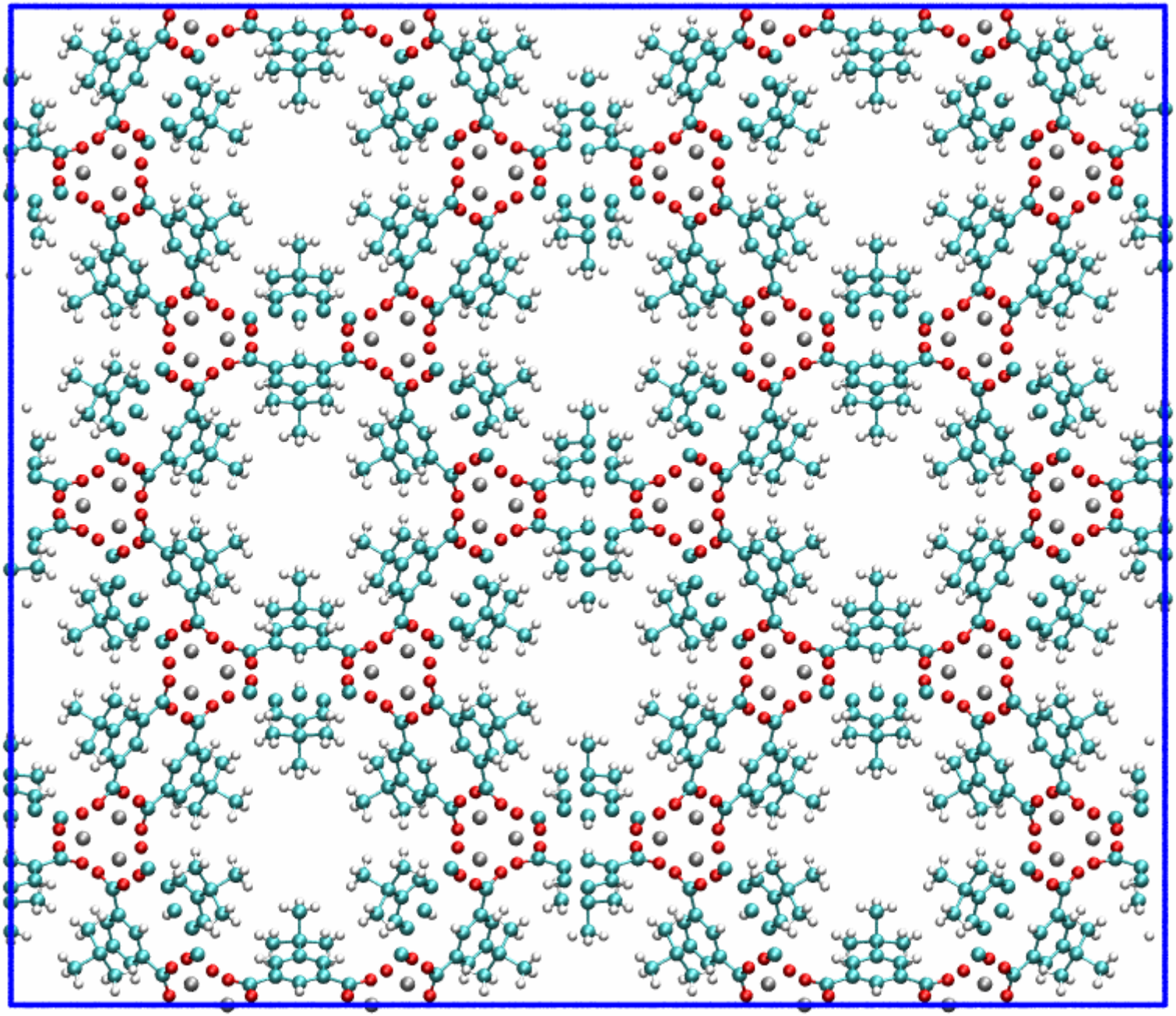

Figure 3

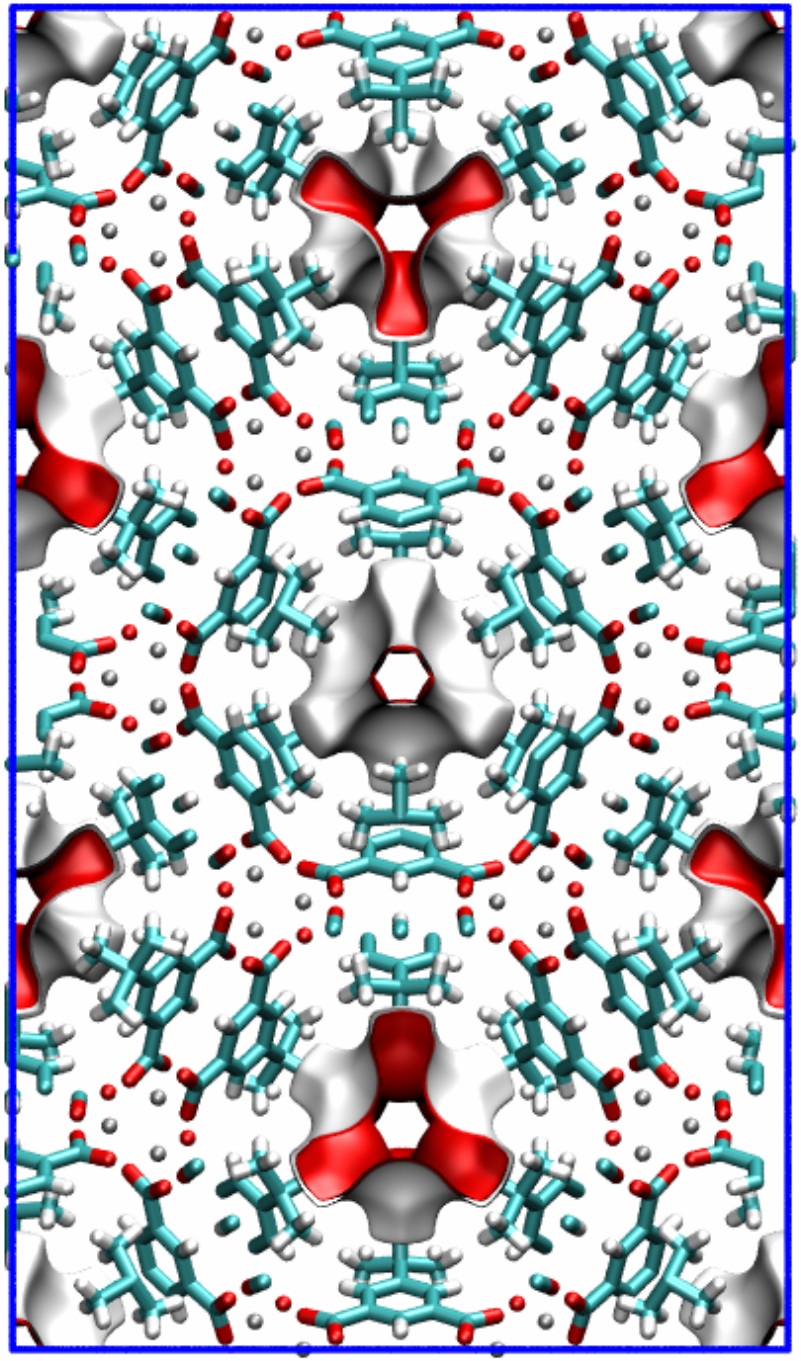

Head-on view of one unit cell of framework; Channels into the paper; The pore landscapes (isopotential surfaces) are shown as the red areas.

Figure 4

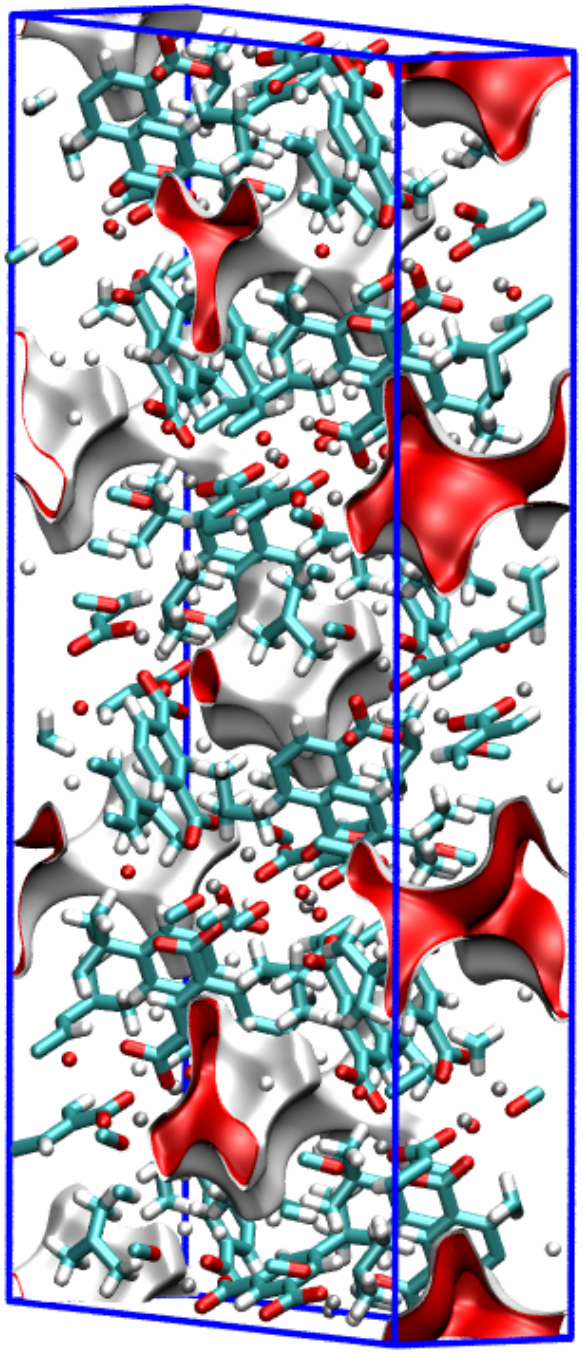

Perspective view of one unit cell of Zn(tbip). One unit cell contains a total of six channel segments. The pore landscapes (isopotential surfaces) are shown as the red areas.

Figure 5

Snapshots showing the location of ethane molecules in Zn(tbip) at 300 K;
Loading = 6 molecules per unit cell

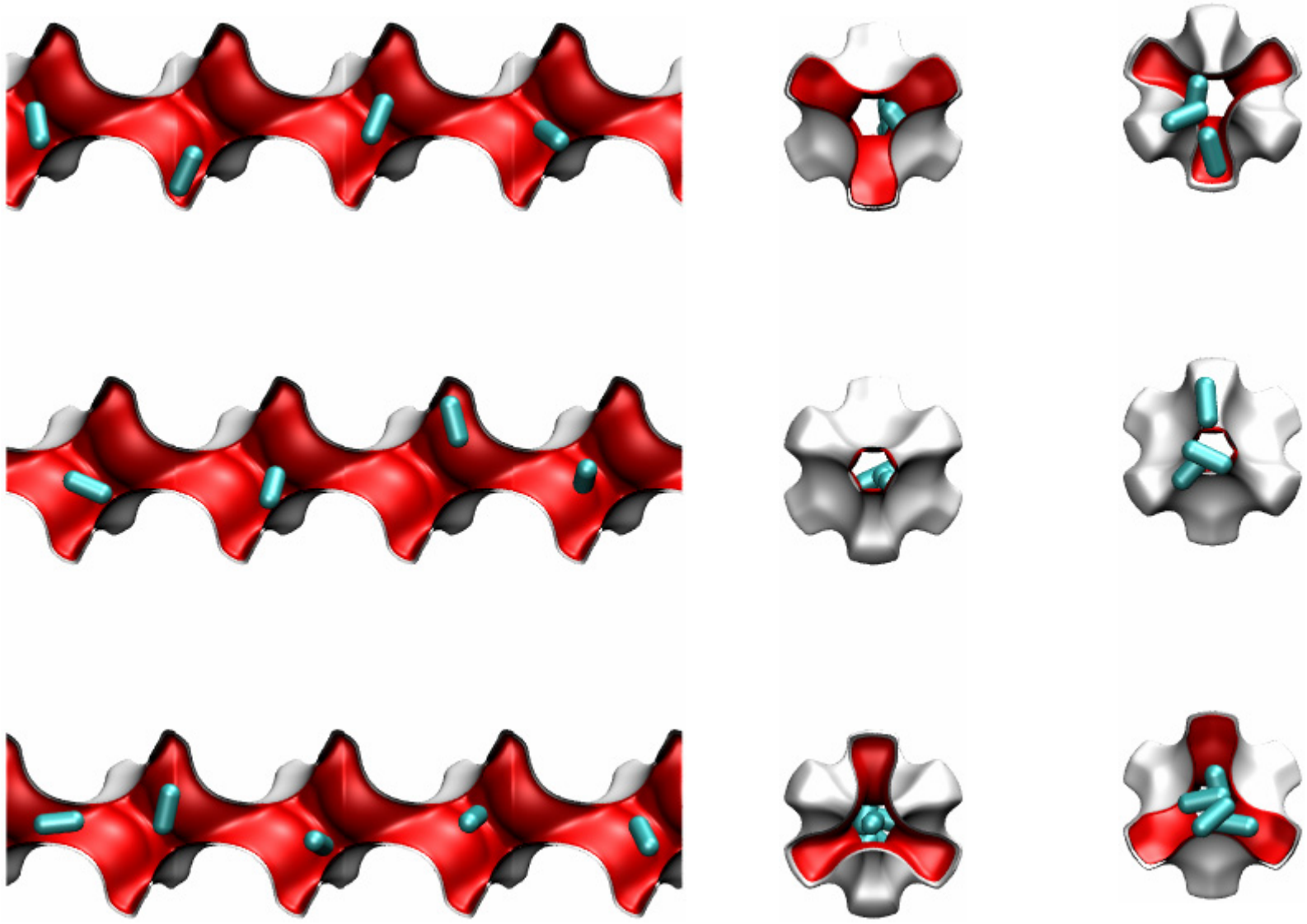

Figure 6

Snapshots showing the location of ethane molecules in Zn(tbip) at 300 K;
Loading = 8 molecules per unit cell

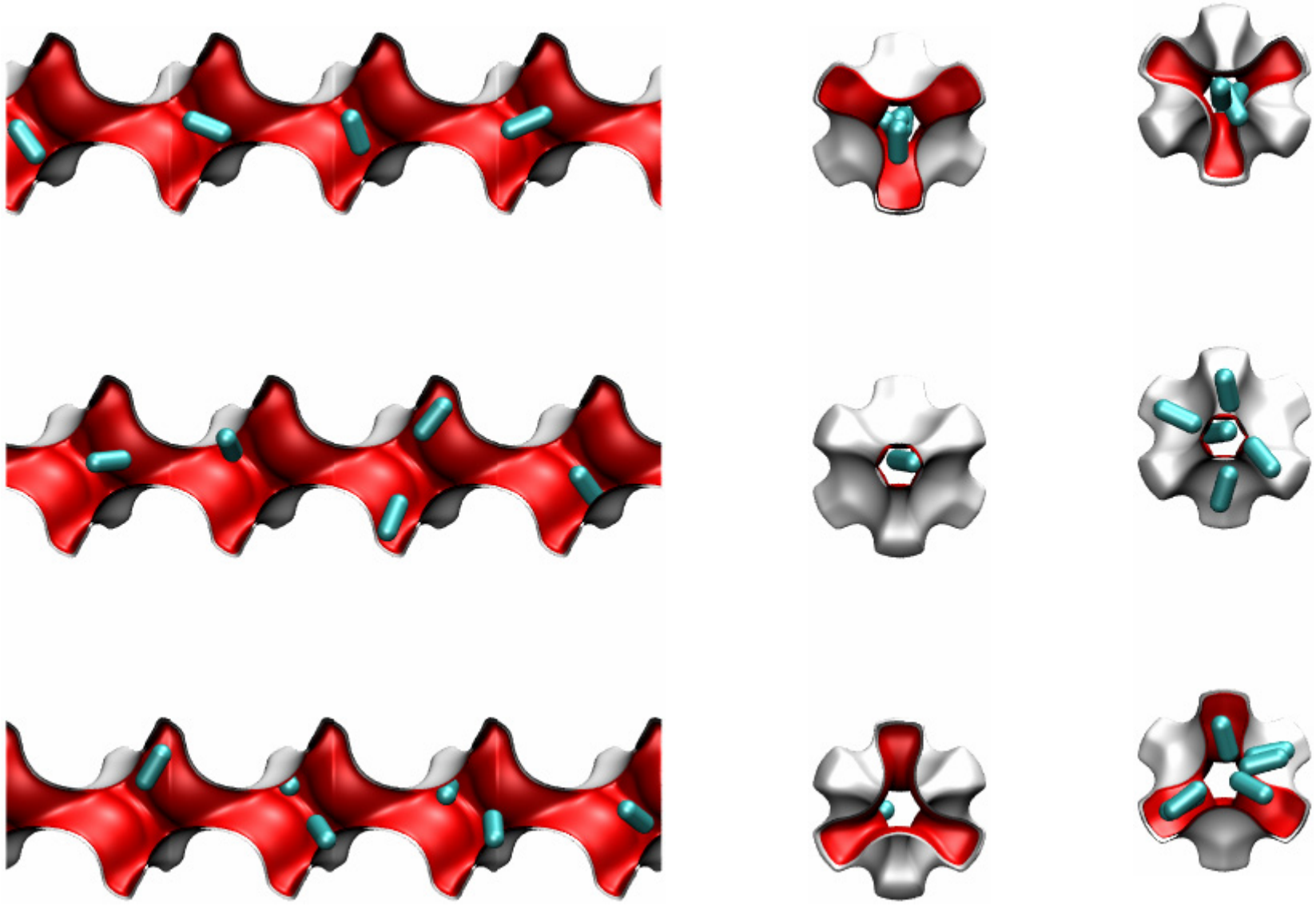

Figure 7

Snapshots showing the location of ethane molecules in Zn(tbip) at 300 K;
Loading = 12 molecules per unit cell

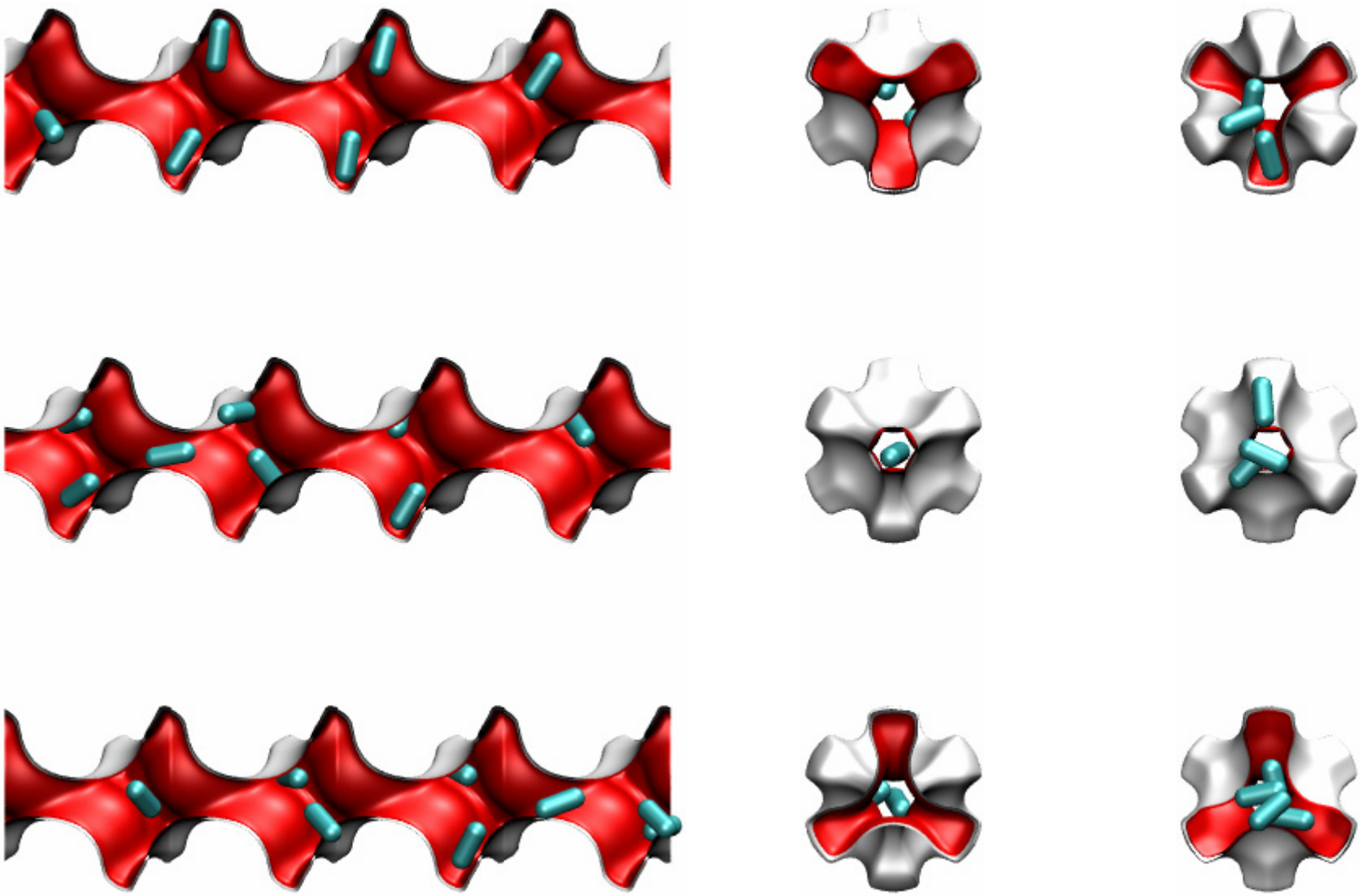

Figure 8

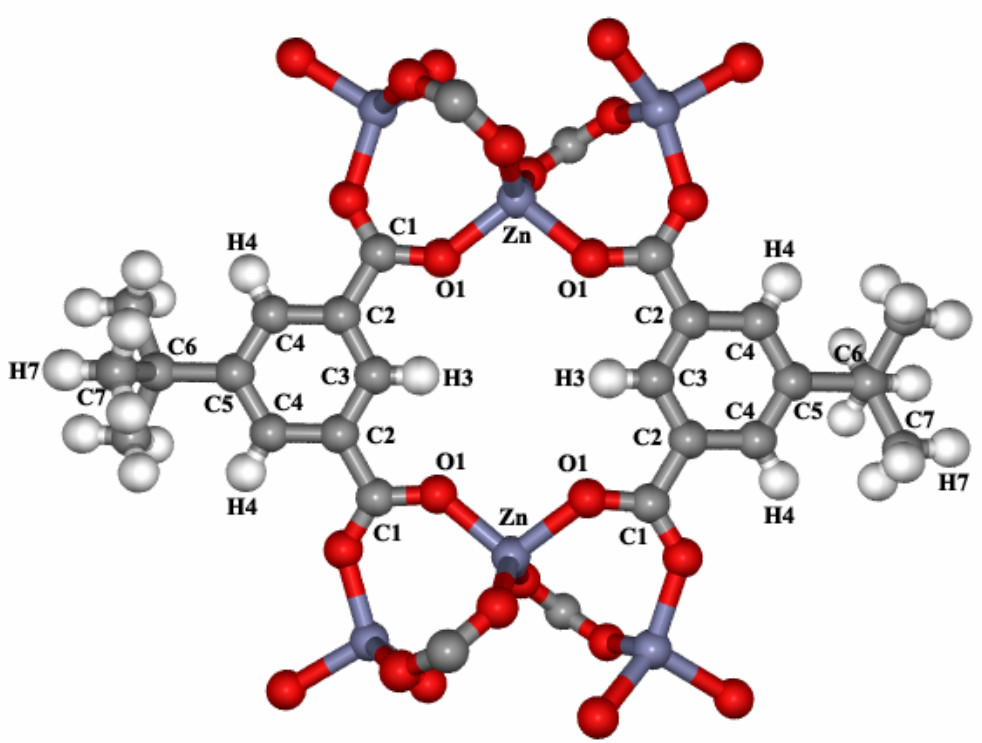
C1
Zn
H4
O1
O1
H4
C2
C2
C6
C4
C4
C6
H7
C7
C5
C4
C3
H3
H3
C3
C4
C5
C7
C2
C2
O1
O1
H7
H4
H4
C1
Zn
C1

Figure 9

Location of a C2 molecule tracked every 0.5 ps during a simulation period of 10 ns. The lattice is flexible.

3.2 molecules per uc

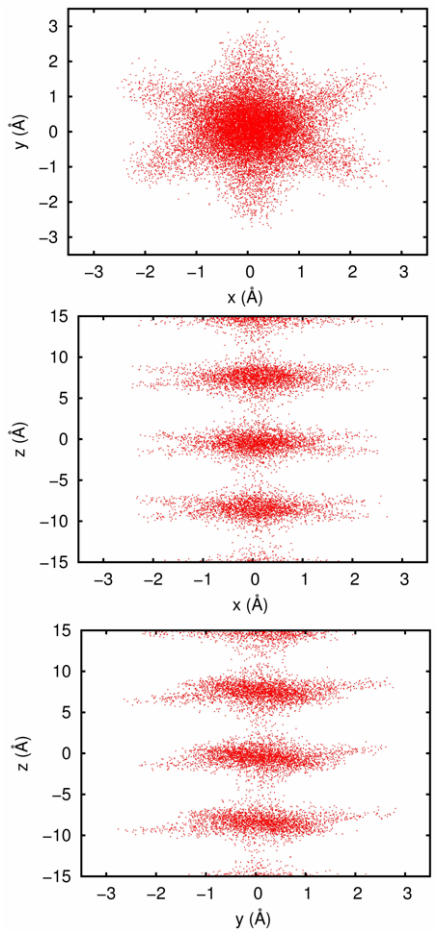

8.4 molecules per uc